

# Supporting Information:

## Removal of Human Leukemic Cells from Peripheral Blood Mononuclear Cells by Cell Recognition Chromatography with Size Matched Particle Imprints

Rosie Chester,<sup>a</sup> Anupam A.K. Das,<sup>a</sup> Jevan Medlock,<sup>a</sup> Dieter Nees,<sup>b</sup>  
David J. Allsup,<sup>c</sup> Leigh A. Madden,<sup>d</sup> and Vesselin N. Paunov\*<sup>a</sup>

<sup>a</sup> Department of Chemistry and Biochemistry, University of Hull, Hull, HU67RX, UK;

<sup>b</sup> Joanneum Research FmbH, Leonhardstrasse 59, 8010 Graz, Austria;

<sup>c</sup> Hull York Medical School, University of Hull, Hull, HU67RX, Hull, HU67RX, UK;

<sup>d</sup> Department of Biomedical Sciences, University of Hull, Hull, HU67RX, UK;.

\* Corresponding author contact details: Phone: +44(0)1482 465660,

Email: [v.n.paunov@hull.ac.uk](mailto:v.n.paunov@hull.ac.uk)

(ACS Applied Bio Materials 2020)

### CONTENTS

Preparation steps of shims for CA15 imprint replication.....	2
R2R Nano-Imprinting Lithography for large scale CA15 imprint replication.....	3
Fabrication protocols for CA15 particle imprints.....	3
Surface modification protocols for CA15 particle imprints.....	3
Optical and SEM images of CA15 imprints.....	4
Total cell count of the HL60/PBMCs circulated over 12 cm CA15 imprints at different bPEI surface treatment concentrations.....	4
Comparison between live and fixed HL60 cells.....	5
Flow velocities, residence times and Reynolds numbers.....	6
Calculated HL60 and PBMC sedimentation velocities and pathway lengths.....	7
References.....	7

This document is the Accepted Manuscript version of a Published Work that appeared in final form in ACS Applied Bio Materials, copyright © American Chemical Society after peer review and technical editing by the publisher. To access the final edited and published work see <https://doi.org/10.1021/acsabm.9b00770>

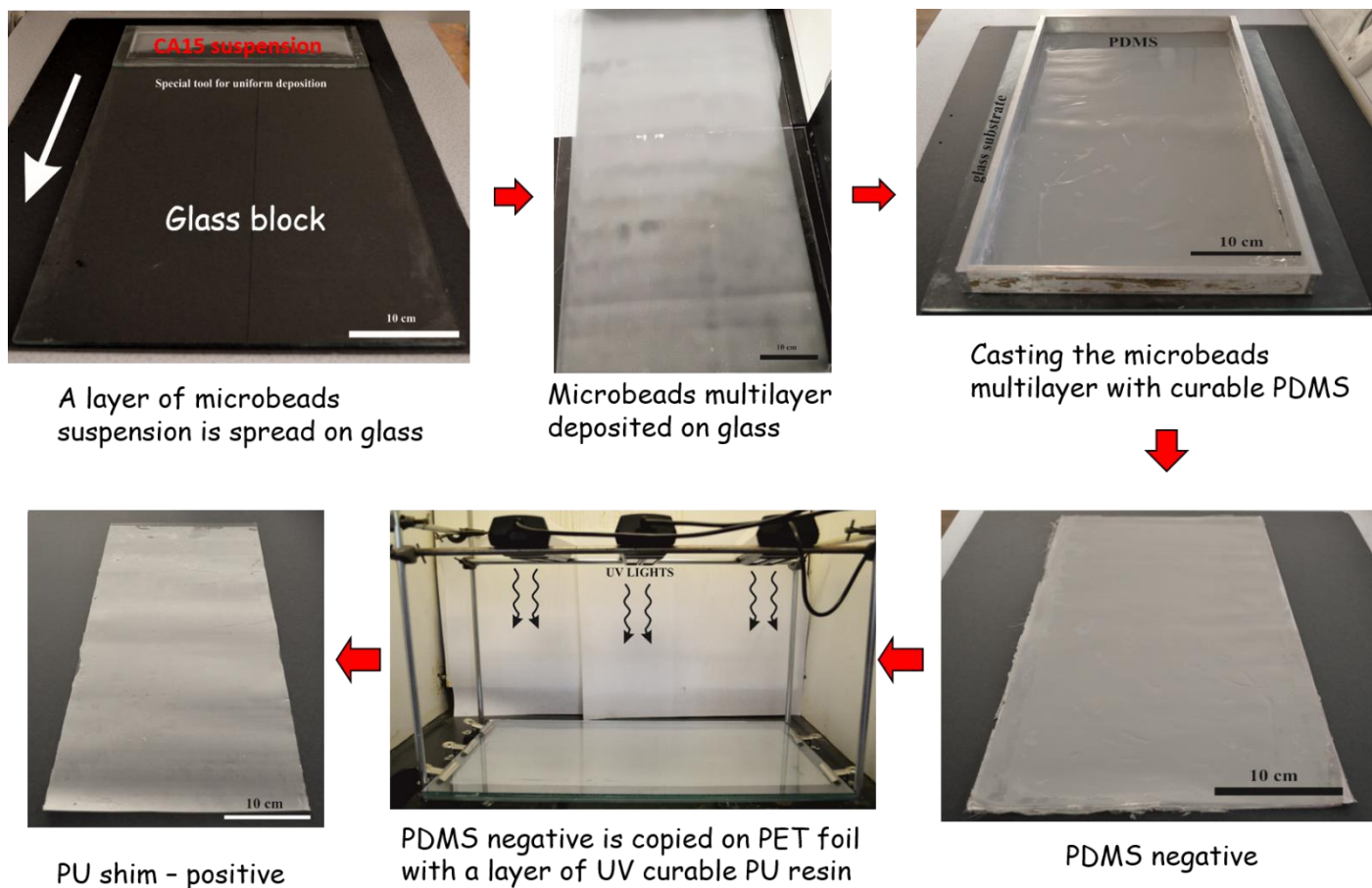


**Figure S1.** Preparation steps for positive imprints (shims) of CA15 microbead layers. The CA15 microbeads suspension is spread on a glass block using a spreading tool consisting of rectangular glass frame which is filled with the microbeads suspension and dragged along the glass surface. The microbeads multilayer is then left to dry in air and then casted with curable PDMS. After curing for 2 days at room temperature, the cured PDMS layer (negative imprint) is peeled off and cleaned by washing with water and detergent. The PDMS negative imprint is then replicated with a layer of UV curable polyurethane resin on PET foil which is cured under UV light (365 nm, 10W) for 10 min to produce a positive CA15 imprint. This mater imprint is used for Roll-to-Roll Nanoimprinting lithography for replication on a very large scale (See Figure S2).

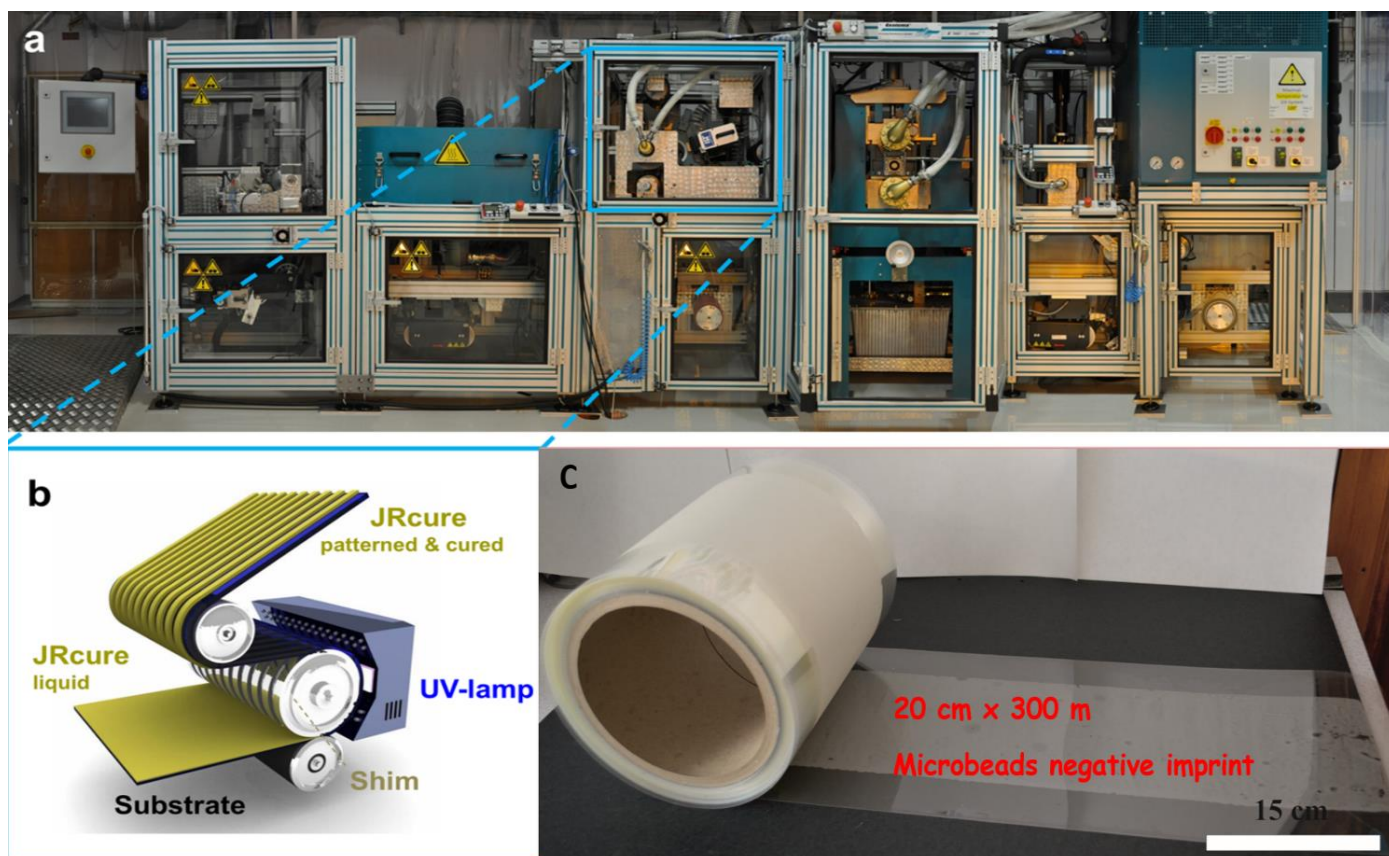


**Figure S2** (a) The Roll-to-Roll-UV Nano-Imprinting Lithography (NIL) machine at our collaborator Joanneum Research FmbH (Weiz, Austria) printing facility with a speed up to  $30 \text{ m min}^{-1}$ . (b) Scheme of the R2R-UV-NIL unit.<sup>1</sup> Photographs showing the production of (c) a roll of negative acrylate-based bioimprint on PET foil fabricated from positive PU imprint shims on PET foil produced with a speed of  $1 \text{ m min}^{-1}$ . Figures S2a and S2b reprinted with permission from ref. 1. Copyright 2016 American Chemical Society.

### Fabrication protocol for CA15 particle imprints

The positive shim imprint (Figure S1) was made using an elastic resin formulated with a PU-acrylate oligomer, two acrylate diluents, a photo-initiator (3 wt%) and a polythiol (10 wt%) for suppressing the  $\text{O}_2$ -inhibition (from the air/ $\text{O}_2$  dissolved in PDMS). The UV curable resin for the final R2R negative imprint contains a hydrophilic acrylate, a photo-initiator (3 wt%) and a silicone surfactant (1 wt%) for easy demolding. The compositions of the resins are proprietary of Joanneum Research FmbH (Weiz, Austria). The imprint base was a PET foil sourced from DuPont Melinex ST505 of thickness  $125 \mu\text{m}$ .

### Surface modification protocol for CA15 particle imprints

The negative CA15 imprint was treated with oxygen-plasma and then coated with branched polyethylene imine (bPEI). It is known that bPEI has certain low toxicity when used as gene-transfer vector in solution. This has been widely researched and commented on by a number of authors<sup>2,3</sup> for multiple cell types exposed to a solution of bPEI. The same polymer has been extensively used for coating nanocarriers for delivery of chemotherapeutic agents due to its relatively low toxicity.<sup>4</sup> However, in the case of our bPEI surface treated imprints, there was no free bPEI in the solution as bPEI is bound to the bioimprint. The CA15 imprint surface is further treated with the Pluronic surfactant Poloxamer 407 which is routinely used for passivation of surfaces in biomedical equipment (catheters, etc.) exposed to biological fluids to minimise non-specific adsorption of cells and biopolymers. Hence during the imprint selectivity experiments, the PBMCs do not come in direct contact with bPEI which may otherwise potentially impact their viability in solution. In our selectivity experiments, however, all cells were fixed for the purposes of preserving their shape and size, hence there is no issue of cell viability loss during circulation.

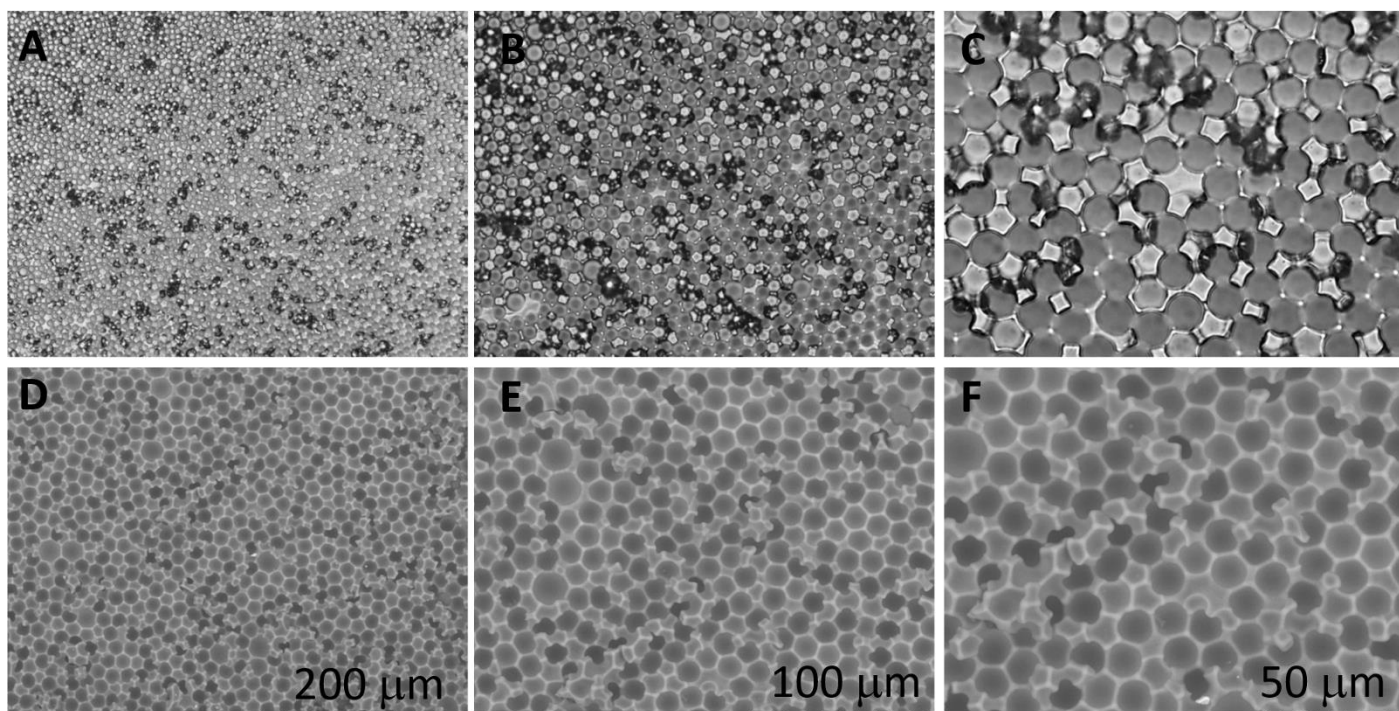


**Figure S3** (a) Optical microscopy images (A)-(C) and SEM images (D)-(F) of CA15 negative particle imprints at different magnifications. Images A and D, B and E, C and F share the same scale bars.

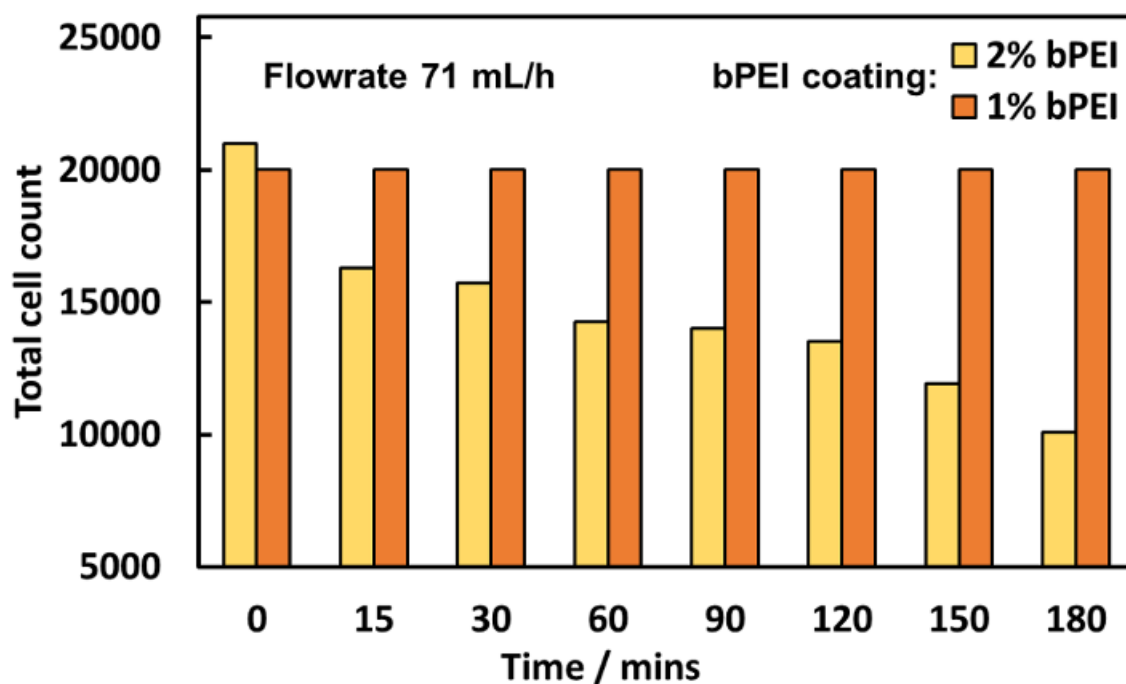


**Figure S4.** Total cell count for the HL60/PBMCs mixture circulating through the imprint chip over 12 cm CA15 imprint at a flow rate of 71 mL/h for channel depth of 250 μm as a function of time. The CA15 particle imprints were treated subsequently with oxygen plasma and two different concentrations of bPEI (1 wt% and 2 wt%) followed by 1 wt% Poloxamer 407. The data are derived from samples taken periodically analyzed by FACS.

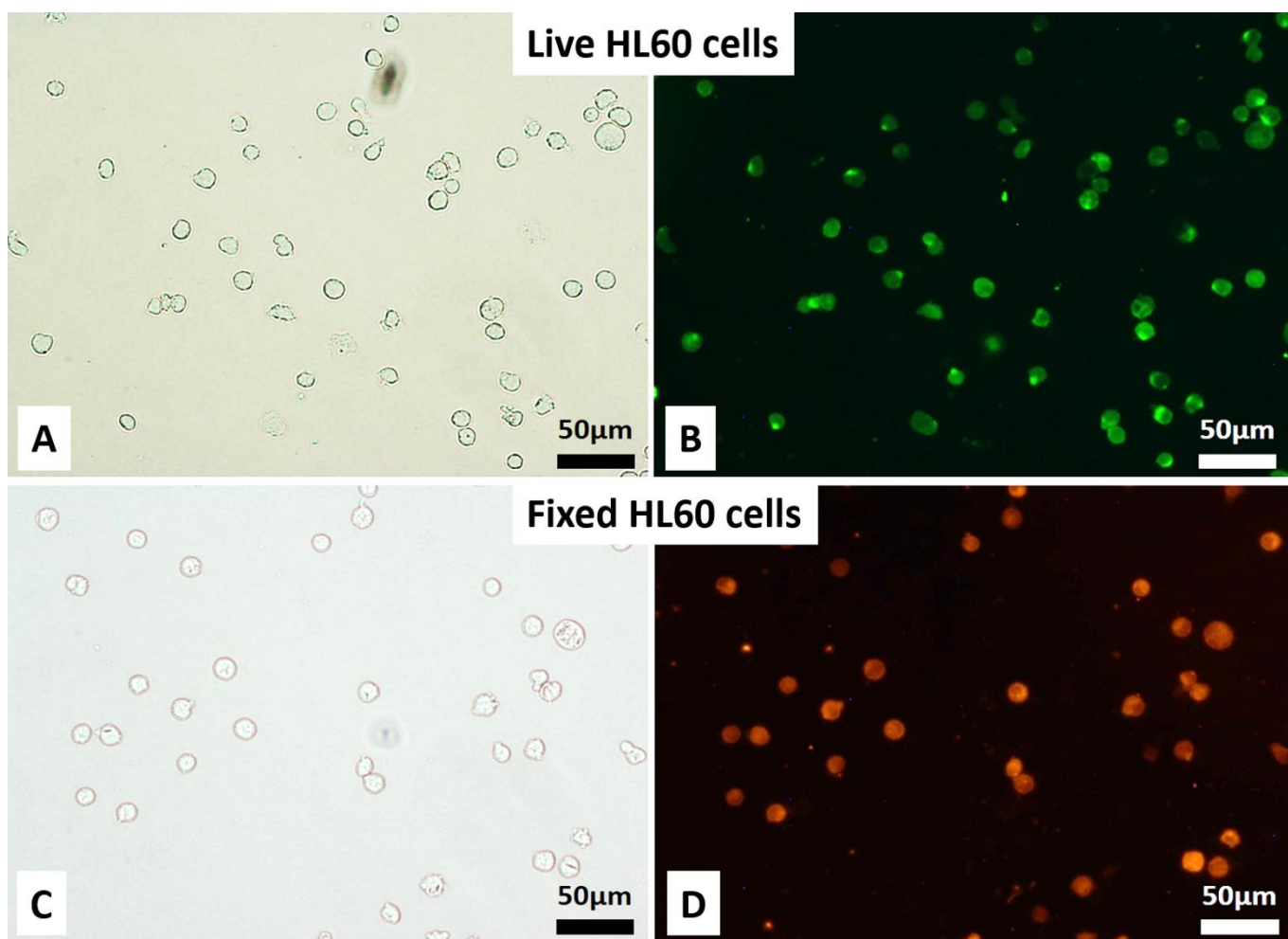


**Figure S5** (A) Optical microscopy image (bright field) and (B) fluorescence microscopy image of live HL60 cells (green) stained using carboxyfluorescein-phospholipid conjugate. (C) Optical microscopy image (bright field) and (D) fluorescence microscopy image of fixed HL60 cells (red) stained using Lissamine Rhodamine sulfonyl B.

The experimental challenge in performing of the cell shape chromatography experiments with live cells is in keeping the cell viability constant throughout the experiment for accounting purposes, rather than the experiment itself, which is exactly the same for live and fixed cells. The potential differences may arise when cells dye and change their shape and size (e.g. deflate) during the experiment. As we cannot control the cell viability in flow-through conditions which take a long time and have batch to batch variations, for the sake of simplicity we did the experiments with fixed cells (both HL60 and PBMCs). We have demonstrated that there is no substantial change of the shape and size of the live HL60 cells before and after fixing (see Figure S5, Supporting Information). The preservation of the cells shape and size is all that matters when it comes to their interaction with the size-matched particle imprint. More detailed studies with live cell systems will be subject to our future research.

**Table S1.** Calculated channel cross-sectional area  $A$ , flow velocity  $v$ , resident time  $t_r$ , the equivalent channel diameter  $D_H$  and the dimensionless Reynolds number  $Re=\rho \times D_H \times v/\eta$  for the flowrates, channel depths and imprint lengths used in our cell recognition experiments.  $Q=A \times v$ ;  $A=d \times w$ ;  $t_r=L/v$ ;  $D_H=4 \times A/P$  with  $P=2(L+d)$  being the average perimeter of the channel cross-section. Here  $\eta=1.05 \times 10^{-3}$  Pa s is the viscosity of the aqueous media (PBS, 25 °C). Here  $w=0.50$  cm is the channel width.

Flowrate $Q$ (mL/h)	Channel depth $d$ ( $\mu\text{m}$ )	Channel length $L$ (cm)	Cross- sectional area $A$ ( $\text{m}^2$ )	Flow velocity $v$ (m/s)	Resident time $t_r$ (s)	Equivalent channel diameter $D_H$ (m)	Reynolds Number
71	125	4	6.25E-07	3.16E-02	1.27E+00	2.4E-04	7.4
95	125	4	6.25E-07	4.22E-02	9.47E-01	2.4E-04	9.9
140	125	4	6.25E-07	6.22E-02	6.43E-01	2.4E-04	14.6
71	125	8	6.25E-07	3.16E-02	2.54E+00	2.4E-04	7.4
95	125	8	6.25E-07	4.22E-02	1.89E+00	2.4E-04	9.9
140	125	8	6.25E-07	6.22E-02	1.29E+00	2.4E-04	14.6
71	125	12	6.25E-07	3.16E-02	3.80E+00	2.4E-04	7.4
95	125	12	6.25E-07	4.22E-02	2.84E+00	2.4E-04	9.9
140	125	12	6.25E-07	6.22E-02	1.93E+00	2.4E-04	14.6
71	250	4	1.25E-06	1.58E-02	2.54E+00	4.8E-04	7.2
95	250	4	1.25E-06	2.11E-02	1.89E+00	4.8E-04	9.7
140	250	4	1.25E-06	3.11E-02	1.29E+00	4.8E-04	14.3
71	250	8	1.25E-06	1.58E-02	5.07E+00	4.8E-04	7.2
95	250	8	1.25E-06	2.11E-02	3.79E+00	4.8E-04	9.7
140	250	8	1.25E-06	3.11E-02	2.57E+00	4.8E-04	14.3
71	250	12	1.25E-06	1.58E-02	7.61E+00	4.8E-04	7.2
95	250	12	1.25E-06	2.11E-02	5.68E+00	4.8E-04	9.7
140	250	12	1.25E-06	3.11E-02	3.86E+00	4.8E-04	14.3
71	500	4	2.50E-06	7.89E-03	5.07E+00	9.1E-04	6.9
95	500	4	2.50E-06	1.06E-02	3.79E+00	9.1E-04	9.2
140	500	4	2.50E-06	1.56E-02	2.57E+00	9.1E-04	13.6
71	500	8	2.50E-06	7.89E-03	1.01E+01	9.1E-04	6.9
95	500	8	2.50E-06	1.06E-02	7.58E+00	9.1E-04	9.2
140	500	8	2.50E-06	1.56E-02	5.14E+00	9.1E-04	13.6
71	500	12	2.50E-06	7.89E-03	1.52E+01	9.1E-04	6.9
95	500	12	2.50E-06	1.06E-02	1.14E+01	9.1E-04	9.2

**Table S2.** Calculated HL60 and PBMC sedimentation velocities,  $u_s = (\rho_c - \rho_m)gD_c^2 / (18\eta)$  and sedimentation pathway lengths  $l_s = t_r \times u_s$  over the residence time for different combinations of flowrates, channel depths and imprint lengths used in our cell recognition experiments. Here  $\rho_c = 1125 \text{ kg m}^{-3}$  is the average cell mass density,  $\rho_m = 1010 \text{ kg m}^{-3}$  is the aqueous media mass density,  $\eta = 1.05 \times 10^{-3} \text{ Pa s}$  is the viscosity of the aqueous media (PBS at 25 °C),  $g = 9.81 \text{ m s}^{-2}$  is the gravity acceleration and  $D_c = 14.5 \mu\text{m}$  is the average cell diameter for HL60 cells and  $D_c = 9.0 \mu\text{m}$  for PBMCs. Here  $w = 0.50 \text{ cm}$  is the channel width.

Flowrate Q (mL/h)	Channel depth d (um)	Channel length L (cm)	HL60 sedimentation velocity $u_s$ / flow velocity v	PBMC sedimentation velocity $u_s$ / flow velocity v	HL60 sedimentation length/channel depth	PBMC sedimentation length/channel depth
71	125	4	4.0E-04	1.5E-04	1.3E-01	4.9E-02
95	125	4	3.0E-04	1.1E-04	9.5E-02	3.7E-02
140	125	4	2.0E-04	7.8E-05	6.5E-02	2.5E-02
71	125	8	4.0E-04	1.5E-04	2.5E-01	9.8E-02
95	125	8	3.0E-04	1.1E-04	1.9E-01	7.3E-02
140	125	8	2.0E-04	7.8E-05	1.3E-01	5.0E-02
71	125	12	4.0E-04	1.5E-04	3.8E-01	1.5E-01
95	125	12	3.0E-04	1.1E-04	2.9E-01	1.1E-01
140	125	12	2.0E-04	7.8E-05	1.9E-01	7.5E-02
71	250	4	8.0E-04	3.1E-04	1.3E-01	4.9E-02
95	250	4	5.9E-04	2.3E-04	9.5E-02	3.7E-02
140	250	4	4.0E-04	1.6E-04	6.5E-02	2.5E-02
71	250	8	8.0E-04	3.1E-04	2.5E-01	9.8E-02
95	250	8	5.9E-04	2.3E-04	1.9E-01	7.3E-02
140	250	8	4.0E-04	1.6E-04	1.3E-01	5.0E-02
71	250	12	8.0E-04	3.1E-04	3.8E-01	1.5E-01
95	250	12	5.9E-04	2.3E-04	2.9E-01	1.1E-01
140	250	12	4.0E-04	1.6E-04	1.9E-01	7.5E-02
71	500	4	1.6E-03	6.1E-04	1.3E-01	4.9E-02
95	500	4	1.2E-03	4.6E-04	9.5E-02	3.7E-02
140	500	4	8.1E-04	3.1E-04	6.5E-02	2.5E-02
71	500	8	1.6E-03	6.1E-04	2.5E-01	9.8E-02
95	500	8	1.2E-03	4.6E-04	1.9E-01	7.3E-02
140	500	8	8.1E-04	3.1E-04	1.3E-01	5.0E-02
71	500	12	1.6E-03	6.1E-04	3.8E-01	1.5E-01
95	500	12	1.2E-03	4.6E-04	2.9E-01	1.1E-01

## References

1. Leitgeb, M.; Nees, D.; Ruttloff, S.; Palfinger, U.; Götz, J.; Liska, R.; Belegriatis, M.R.; Stadlober, B.; Multilength Scale Patterning of Functional Layers by Roll-to-Roll Ultraviolet-Light-Assisted Nanoimprint Lithography, *ACS Nano*, **2016**, *10*, 4926-4941.
2. Kafil, V.; Omid, Y.; Cytotoxic impacts of linear and branched polyethylenimine nanostructures in a431 cells, *Bioimpacts*, **2011**, *1*, 23-30.
3. Castan, L.; da Silva, C.J.; Molina, E.F.; dos Santos, R.A.; Comparative study of cytotoxicity and genotoxicity of commercial Jeffamines® and polyethylenimine in CHO-K1 cells, *J. Biomed. Mater. Res. B: Appl. Biomater.*, **2018**, *106B*, 742-750.
4. Din, F.U.; Aman, W.; Ullah, I.; Qureshi, O.S.; Mustapha, O.; Shafique, S.; Zeb, A.; Effective use of nanocarriers as drug delivery systems for the treatment of selected tumors. *Int. J. Nanomed.* 2017, **12**, 7291–7309.